livers

MDPI

Article

Integrative Profiling of Metabolic *CYP* Expression, DNA Mutation Rates, and Immune Cell Infiltration for Survival Prognosis in Hepatocellular Carcinoma

Mona Dawood [1,2], Axel Guthart [1], Ednah Ooko [3,4], Ralf Weiskirchen [5], Thomas Efferth [1] and Joelle C. Boulos [1,*]

[1] Department of Pharmaceutical Biology, Institute of Pharmaceutical and Biomedical Sciences, Johannes Gutenberg University, Staudinger Weg 5, 55128 Mainz, Germany; modawood@uni-mainz.de (M.D.); efferth@uni-mainz.de (T.E.)
[2] Department of Molecular Biology, Faculty of Medical Laboratory Science, Al-Neelain University, Khartoum 12702, Sudan
[3] Laboratory of Cell Biology, Center for Cancer Research, National Cancer Institute, National Institutes of Health, Bethesda, MD 20892, USA; ednah.ooko@nih.gov
[4] Department of Biological Sciences, School of Natural and Applied Sciences, Masinde Muliro University of Science and Technology, Kakamega 50100, Kenya
[5] Institute of Molecular Pathobiochemistry, Experimental Gene Therapy and Clinical Chemistry (IFMPEGKC), RWTH University Hospital Aachen, 52074 Aachen, Germany; rweiskirchen@ukaachen.de
* Correspondence: joboulos@uni-mainz.de

Abstract

Background/Objectives: Hepatocellular carcinoma (HCC) is challenging to treat with chemotherapy. Immunotherapy has shown moderate responses in inflammatory and immunosuppressive tumor environments. Hepatic cytochrome P450 monooxygenases (CYPs) play a crucial role in xenobiotic and drug metabolism, as well as lipid and steroid metabolism. We aimed to investigate whether *CYP* expression and various parameters of the innate and adaptive immune system are prognostic factors for the survival of HCC patients. Methods: HCC biopsies ($n = 370$) from The Cancer Genome Atlas (TCGA) database were analyzed using Kaplan–Meier statistics and the KMPlotter algorithm. Parameters such as immune cell infiltration, DNA mutation rates, and neoantigen load were selected for survival analysis and subjected to hierarchical cluster analysis. The expression of candidate *CYP* genes in tumors was compared to that in normal liver tissues. Furthermore, tumor infiltration of innate immune cells (basophilic and eosinophilic granulocytes, natural killer cells), adaptive immune cells (CD4+ memory and CD8+ cytotoxic T cells, regulatory T cells, type 1 and type 2 helper T cells), and mesenchymal stem cells was examined. Results: High expression of *CYP19A1* and *CYP26B1* was associated with shorter survival, whereas high expression of *CYP3A5*, *CYP3A43*, *CYP7A1*, and *CYP27A1* was linked to longer survival. Mutation rates combined with *CYP* expression showed a correlation with five out of six *CYP* genes, while a high neoantigen load produced less definitive results. A specific cluster exhibiting high *CYP* expression and immune cell counts or mutation/neoantigen rates was associated with shorter survival, while another cluster was linked to longer survival. Conclusions: CYPs involved in the metabolic regulation of HCC, including *CYP3A5*, *CYP3A43*, *CYP7A1*, *CYP19A1*, *CYP26B1*, and *CYP27A1*, were found to have prognostic value for patient survival. Combined signatures that include *CYP* expression, mutational rates, and immune cell infiltration into tumors further enhanced the prognostic value for patient survival. This suggests that CYPs may influence the creation of a tumor-specific metabolic microenvironment that impacts immune functions. These combined signatures could be utilized for patient stratification to personalize tumor treatment and develop

Check for updates

Academic Editor: Hartmut W. Jaeschke

Received: 12 March 2026
Revised: 14 May 2026
Accepted: 22 May 2026
Published: 9 June 2026

Copyright: © 2026 by the authors. Licensee MDPI, Basel, Switzerland. This article is an open access article distributed under the terms and conditions of the Creative Commons Attribution (CC BY) license.

novel combination therapies aimed at optimizing treatment outcomes, such as combining transarterial chemoembolization (TACE) with immune checkpoint inhibitors.

Keywords: biomarkers; drug treatment; immunotherapy; liver enzymes; patient stratification; prognostic factors

1. Introduction

Hepatocellular carcinoma (HCC) is the most common primary malignant tumor of the liver, accounting for approximately 85–90% of cases. Worldwide, HCC ranks as the sixth to seventh most common cancer, and unfortunately is the third to fourth most common cause of tumor-related death. There is a significant geographical concentration, especially in East Asia (particularly China), Southeast Asia, and sub-Saharan Africa, which may be related to environmental factors. It is not known why men are more frequently affected than women epidemiologically. As a central organ of metabolism in the human body, the prognosis of tumors deriving from the liver is poor, although patients with low-stage tumors live longer than those with higher stages [1,2]. Unfortunately, the outcome is still not satisfactory for the majority of patients despite considerable progress that has been made in the management of HCC during the past years.

In the vast majority of cases, HCC develops based on existing liver cirrhosis. The most crucial etiological risk factors include chronic hepatitis B virus (HBV) and hepatitis C virus (HCV) infections. Although hepatitis virus infections are among the most frequently found causes, other causes include alcoholic cirrhosis, non-alcoholic fatty liver disease (NAFLD), and non-alcoholic steatohepatitis (NASH), which are frequently underestimated. Furthermore, exposure to aflatoxin B1 from mold also plays an important role in other regions [3]. Additionally, genome-wide association analysis (GWAS) revealed that genetic factors predisposing to the metabolic syndrome also increase the risk of HCC [4,5].

At the molecular level, hepatocarcinogenesis is characterized by aberrant signal transduction pathways due to mutations in key genes, e.g., *TP53* and β-catenin mutations and deregulated signaling pathways such as PI3K/AKT/MTOR, RAS/MAPK, IGF, HGF/MET, VEGF, EGFR, and PDGF [6,7]. Immune escape due to dysregulated interleukin and transforming growth factor β (TGF-β) signaling represents another factor for liver cancer development [8]. These factors are considered both as diagnostic biomarkers and targets for targeted therapies and immuno-oncological treatment approaches.

Classic systemic intravenous chemotherapy is hardly effective in HCC due to inherent chemoresistance. Curative treatment attempts are only applied in the early stages of the disease. These include surgical liver resection, local ablation procedures (radiofrequency ablation (RFA) and microwave ablation (MWA)), and—in selected cases—liver transplantation. However, which options are available when curative measures are no longer successful? Possible approaches are the locoregional treatment methods. In transarterial chemoembolization (TACE), chemotherapeutic agents (doxorubicin, epirubicin, or cisplatin) are selectively given via the hepatic artery, followed by vessel embolization as postoperative adjuvant therapy. The advantage of this technique compared to standard chemotherapy is that the ischemic effect reached by vessel embolization enhances the cytotoxic effects of the chemotherapeutic drugs. Another method is transarterial radioembolization or selective internal radiotherapy (TARE/SIRT), where yttrium-90-loaded microspheres are introduced into the tumor area for local radiation applications. Systemic therapy is reserved for advanced or locally untreatable diseases [9,10]. In first-line treatment, the combination of the PD-L1 antibody atezolizumab and the VEGF antibody bevacizumab is considered standard

therapy [11]. Alternatively, tyrosine kinase inhibitors such as lenvatinib or sorafenib are used. Additional targeted substances like regorafenib, cabozantinib, and the VEGF receptor 2 antibody ramucirumab are available as second-line treatments [12–14]. For the majority of patients, these more individualized treatment strategies result in a noticeable slowing of the progression of their disease.

DNA-damaging chemotherapeutic agents can increase somatic mutations and generate new neoantigens. This should theoretically enhance the immunogenicity of a tumor, although this has not always been convincingly demonstrated in clinical practice. Drug-induced DNA damage with an increase in neoantigens creates an interface between chemotherapy and immunotherapy. Some drugs, including anthracyclines and platinum compounds, are known to induce immunogenic cell death by causing DNA double-strand breaks, endoplasmic reticulum stress, and reactive oxygen species (ROS), leading to the release of tumor-associated antigens and the exposure of danger-associated molecular patterns (DAMPs). These signals can trigger antitumor immune responses [15].

HCC cells express specific immunogenic cell death markers following TACE with doxorubicin [16,17]. However, there is currently no clear clinical evidence that anthracycline-induced immunogenic cell death is primarily responsible for the therapeutic success in HCC. A similar effect is observed with platinum derivatives. Oxaliplatin-induced intra- and interstrand crosslinks, defective DNA repair, and mutagenic replication increase tumor antigen presentation and induce immunogenic cell death [18].

One reason for the modest response to immunotherapy alone is the specific tumor microenvironment of HCC, characterized by chronic inflammation and immunosuppression. This environment leads to T cell exhaustion, preventing immunogenic cell death-associated danger signals from triggering an effective adaptive immune response. In response, combination therapies involving loco-regional procedures and immunotherapy have been developed [19]. The hypothesis is that anthracyclines such as doxorubicin induce immunogenic cell death during TACE, while immune checkpoint inhibitors prevent T-cell exhaustion, enhancing the antitumor immune response.

Since standard chemotherapeutics are largely ineffective, immunotherapy inhibiting programmed death-1 (PD-1), programmed death-ligand 1 (PD-L1), and cytotoxic T lymphocyte antigen-4 (CTLA-4) has become a central component of HCC treatment in recent years [20]. Checkpoint inhibitors release key immune brake mechanisms, reactivating tumor-specific T cells. Although only a subset of patients benefits from immunotherapy, with objective response rates of approximately 20–30%, it has significant prognostic value. It provides long-term disease control for responders and offers substantial survival benefits compared to previous systemic therapy approaches.

CYP enzymes (cytochrome P450 monooxygenases) are a family of 57 isoenzymes that play a crucial role in the hepatic phase 1 metabolism of xenobiotics, including cancer drugs and other endogenous substances. Some CYP enzymes can activate carcinogenic substances, while others can degrade them [21]. Interestingly, the metabolism and pharmacokinetics of anthracyclines (e.g., doxorubicin) and tyrosine kinase inhibitors (e.g., sorafenib) are partially dependent on CYP enzymes. CYP enzymes produce ROS and endoplasmic stress, leading to DNA damage [22,23]. This connection between CYP-induced DNA damage, the mutation rate of liver tumors, and their neoantigen load raises the question of whether CYP-mediated metabolism of anticancer drugs increases neoantigen release and triggers immunogenic cell death. First experimental evidence supports this notion [24], although clinical evidence is currently limited and systematic analyses are not yet available. This question needs to be addressed in the future.

This study aimed to investigate the *CYP* expression in HCC and its significance for patient survival. To achieve this, 370 tumor biopsies sequenced as part of The Cancer

Genome Atlas (TCGA) project were analyzed using Kaplan–Meier statistics. Additionally, we examined whether the expression of 35 *CYP* genes, along with mutation rate, neoantigen load, and cell counts of 11 immune cell types, could be prognostically relevant parameters for tumor infiltration. The results indicate that specific CYPs and immune cell infiltration patterns were significant for the overall survival of HCC patients. These findings suggest that these profiles could be considered in the development of novel diagnostic and treatment protocols for personalized therapy.

2. Materials and Methods

2.1. Kaplan–Meier Survival Analysis

We calculated the survival probabilities of patients using the KM Plotter algorithm (https:/www.kmplot.com/analysis) (accessed on 21 January 2026) as previously described [25,26]. The human genome encodes 57 functional *CYP* genes; however, only 35 of them are represented in the KMPlotter database. A total of 370 HCC cases from TCGA were included in the analysis. To avoid type I errors, we used a false discovery rate (FDR) cutoff of 5% [27].

2.2. Cox Regression Analysis

Univariable and multivariable Cox regression analyses were performed to further evaluate the prognostic relevance of the six *CYP* genes identified in the Kaplan–Meier analysis. Overall survival (OS) was the endpoint, and survival time was defined as days-to-death or to the last follow-up. The multivariable models included age, sex, pathological stage, and histological grade. Age was entered as a continuous variable, while the other covariates were treated as categorical variables. Pathological stage was categorized as stage I/II versus stage III/IV, and histological grade as G1/G2 versus G3/G4. Survival and clinical data for the TCGA-LIHC cohort were obtained from the National Cancer Institute Genomic Data Commons (NCI GDC) Data Portal [28], while the corresponding gene expression data were downloaded from UCSC Xena [29]. After merging the survival, clinical, and gene expression data and excluding cases with incomplete or inconsistent information, 325 HCC cases from TCGA cases were evaluated in the main Cox regression analysis. In an additional sensitivity analysis, cirrhosis/fibrosis status was considered using the Ishak fibrosis score as a surrogate. Therefore, Ishak 0–4 was compared to Ishak 5–6. This analysis included 191 evaluable cases. All statistical analyses were performed using IBM SPSS Statistics for Windows version 29.0.2.0 (IBM Corp., Armonk, NY, USA). Hazard ratios are reported with 95% confidence intervals (CI). Forest plots were created using GraphPad Prism 10.4.2 (GraphPad Software, Boston, MA, USA).

2.3. Kaplan–Meier Analysis of CYP Expression and Mutation Status

To investigate whether the prognostic relevance of *CYP* expression varies by mutational background, additional Kaplan–Meier analyses were performed for the genes *TP53* and *CTNNB1*. Both were classified as wildtype or mutated based on the presence of non-synonymous mutations. Mutation status was obtained from UCSC Xena using the TCGA unified ensemble mutation calls [29,30]. The previously used TCGA-LIHC cohort (n = 325), was used, and mutation status was added. For each *CYP*, patients were divided into low- and high-expression groups based on the median. The *CYP* expression group was then combined with *TP53* or *CTNNB1* mutation status, resulting in four groups for each *CYP*/mutation pair. Kaplan–Meier curves were created in SPSS, and groups were compared using the log-rank test.

2.4. Evaluation of CYP Expression and Tumor Immune Cell Infiltration

Spearman correlation coefficient between *CYP* genes and immune-related markers was carried out using GraphPad Prism (GraphPad Software, San Diego, CA, USA). Normalized gene expression from the TCGA database was used. Then, a heatmap was generated using hierarchical clustering of the CIM miner software (https://discover.nci.nih.gov/cimminer/oneMatrix.do) (accessed on 5 May 2026).

Immune infiltration in TCGA does not use direct immunological assays, such as flow cytometry; instead, they apply multiple computational algorithms for the tumor transcriptome profiles. TIMER platform (http://timer.cistrome.org/) uses an R package called immunedeconv with integration of different algorithms such as TIMER, xCell, MCP-counter, CIBERSORT, EPIC, and quanTIseq to estimate the immune infiltration levels for TCGA [31].

These methods have several limitations: (1) TIMER counts immune cells indirectly using the bioinformatics tools that are based on bulk tumor transcriptome profiles. (2) It also lacks the sensitivity to determine the subsets of the immune cells, like T-regulatory subtypes [31].

2.5. Comparison of CYP mRNA Expression in HCC and Normal Liver

The National Cancer Institute (NCI) in the USA conducted the TCGA project, analyzing over 20,000 cancer samples and their corresponding normal tissues from 33 different cancer types. In this study, we examined the mRNA expression levels of six *CYP* genes in 371 HCC samples and 50 normal liver samples using Timer2.0 Cistrome (https://timer.cistrome.org) (accessed on 21 January 2026).

3. Results

3.1. Kaplan–Meier Survival Analyses

Of the 57 functional *CYP* genes in the human genome, the 35 available genes were included in the KMPlotter database (Table 1).

Table 1. *CYP* gene family members were analyzed in the present investigation for their prognostic value in renal cell carcinoma [1].

Symbol	Name	Additional Name	Function	Localization
CYP11A1	Cytochrome P450, family 11, subfamily A, polypeptide 1	Cholesterol side-chain cleavage enzyme, mitochondrial	Catalyzes the conversion of cholesterol to pregnenolone in the synthesis of steroid hormones.	Mit
CYP11B1	Cytochrome P450, family 11, subfamily B, polypeptide 1	Steroid 11-β-hydroxylase	Converts progesterone to cortisol in the adrenal cortex.	Mit
CYP11B2	Cytochrome P450, family 11, subfamily B, polypeptide 2	Aldosterone-synthesizing enzyme	Steroid 18-hydroxylase activity to synthesize aldosterone and 18-oxocortisol; steroid 11β-hydroxylase activity.	Mit

Table 1. *Cont.*

Symbol	Name	Additional Name	Function	Localization
CYP17A1	Cytochrome P450, family 17, subfamily A, polypeptide 1	17-α-Hydroxyprogesterone aldolase	Corticoid and androgen biosynthesis.	ER
CYP19A1	Cytochrome P450, family 19, subfamily A, polypeptide 1	Flavoprotein-linked monooxygenase	Estrogen biosynthesis.	ER
CYP1A1	Cytochrome P450, family 1, subfamily A, polypeptide 1	Aryl hydrocarbon hydroxylase	Metabolizes PAHs to carcinogenic intermediates. Associated with lung cancer risk.	ER
CYP1A2	Cytochrome P450, family 1, subfamily A, polypeptide 2	Cholesterol 25-hydroxylase	Metabolizes some PAHs to carcinogenic intermediates.	ER
CYP1B1	Cytochrome P450, family 1, subfamily B, polypeptide 1	Hydroperoxy icosatetraenoate dehydratase	Metabolizes procarcinogens, e.g., polycyclic aromatic hydrocarbons and 17β-estradiol.	ER
CYP20A1	Cytochrome P450, family 20, subfamily A, polypeptide 1		Iron ion binding and oxidoreductase activity.	N.D.
CYP21A2	Cytochrome P450, family 21, subfamily A, polypeptide 2	Steroid 21-hydroxylase	Synthesis of steroid hormones, e.g., cortisol and aldosterone.	ER
CYP24A1	Cytochrome P450, family 24, subfamily A, polypeptide 1	Vitamin D 24-hydroxylase	Degradation of 1,25-dihydroxyvitamin D3.	Mit
CYP26A1	Cytochrome P450, family 26, subfamily A, polypeptide 1	Retinoic acid 4-hydroxylase	4-Hydroxylation and 18-hydroxylation activities on retinoids, including all-trans-retinoic acid.	ER
CYP26B1	Cytochrome P450, family 26, subfamily B, polypeptide 1	Retinoic acid-metabolizing cytochrome	Inactivation of all-trans retinoic acid to hydroxylated forms.	ER
CYP26C1	Cytochrome P450, family 26, subfamily C, polypeptide 1		Inactivation of all-trans retinoic acid to hydroxylated forms.	N.D.
CYP27A1	Cytochrome P450, family 27, subfamily A, polypeptide 1	5-β-Cholestane-3-α,7-α,12-α-triol 26-hydroxylase	Oxidizes cholesterol intermediates as part of the bile synthesis pathway.	Mit
CYP27B1	Cytochrome P450, family 27, subfamily B, polypeptide 1	25-Hydroxyvitamin D3 1α-hydroxylase	Hydroxylates 25-hydroxyvitamin D3 at the 1α position.	Mit
CYP27C1	Cytochrome P450, family 27, subfamily C, polypeptide 1	All-trans retinol 3,4-desaturase	Iron ion binding and oxidoreductase activity.	N.D.

Table 1. *Cont.*

Symbol	Name	Additional Name	Function	Localization
CYP39A1	Cytochrome P450, family 39, subfamily A, polypeptide 1	Oxysterol 7-α-hydroxylase	Substrates include the oxysterols 25-hydroxycholesterol, 27-hydroxycholesterol, and 24-hydroxycholesterol.	ER
CYP3A4	Cytochrome P450, family 3, subfamily A, polypeptide 4	Glucocorticoid-inducible P450	Metabolism of approximately half the drugs in use today, including acetaminophen, codeine, cyclosporin A, diazepam, erythromycin, and chloroquine. The enzyme also metabolizes some steroids and carcinogens.	ER
CYP3A43	Cytochrome P450, subfamily IIIA, polypeptide 43		Hydroxylates testosterone; role in aging mechanisms and cancer progression.	N.D.
CYP3A5	Cytochrome P450, family 3, subfamily A, polypeptide 5		Metabolizes drugs and steroid hormones (testosterone and progesterone).	N.D.
CYP3A7	Cytochrome P450, family 3, subfamily A, polypeptide 5	Xenobiotic monooxygenase	Hydroxylates testosterone and dehydroepiandrosterone 3-sulfate in estriol formation during pregnancy.	N.D.
CYP46A1	Cytochrome P450, Family 46, Subfamily A, Polypeptide 1	Cholesterol 24S-hydroxylase	Converts cholesterol to 24S-hydroxycholesterol.	ER
CYP4A11	Cytochrome P450, family 4, subfamily A, polypeptide 11	Long-chain fatty acid ω-monooxygenase	Hydroxylates medium-chain fatty acids, e.g., laurate and myristate.	ER
CYP4A22	Cytochrome P450, family 4, subfamily A, polypeptide 22	Long-chain fatty acid ω-monooxygenase	Hydroxylates medium-chain fatty acids, e.g., laurate and myristate.	ER
CYP4B1	Cytochrome P450, family 4, subfamily B, polypeptide 1	Cytochrome P450-HP	Metabolizes specific carcinogens.	ER
CYP4F11	Cytochrome P450, family 4, subfamily F, polypeptide 11	Phylloquinone ω-hydroxylase	Metabolizes fatty acids and catalyzes N- and O-demethylation of specific drugs.	N.D.
CYP4F12	Cytochrome P450, family 4, subfamily F, polypeptide 12		Catalyzes the epoxidation of 22:6n-3 and 22:5n-3 polyunsaturated long-chain fatty acids; oxidizes arachidonic acid.	ER

Table 1. *Cont.*

Symbol	Name	Additional Name	Function	Localization
CYP4F2	Cytochrome P450, family 4, subfamily F, polypeptide 2	Leukotriene-B(4) ω-hydroxylase 1	Degrades leukotriene B4 (inflammation mediator).	ER
CYP4F22	Cytochrome P450, family 4, subfamily F, polypeptide 22	Ultra-long-chain fatty acid ω-hydroxylase	Role in the 12(R)-lipoxygenase pathway (inflammation mediator).	N.D.
CYP4F3	Cytochrome P450, family 4, subfamily F, polypeptide 3	Leukotriene B4 ω hydroxylase	Degrades leukotriene B4 (inflammation mediator).	ER
CYP51A1	Cytochrome P450, family 51, subfamily A, polypeptide 1	Lanosterol 14-α demethylase	Participates in the synthesis of cholesterol by catalyzing the removal of the 14α-methyl group from lanosterol.	ER
CYP7A1	Cytochrome P450, family 7, subfamily A, polypeptide 1	Cholesterol 7α-hydroxylase	Converts cholesterol to bile acids.	ER
CYP7B1	Cytochrome P450, family 7, subfamily B, polypeptide 1	25-Hydroxycholesterol 7-α-hydroxylase	Converts cholesterol to bile acids.	ER
CYP8B1	Cytochrome P450, family 8, subfamily B, polypeptide 1	7-α-Hydroxycholest-4-en-3-one 12-α-hydroxylase	Catalyzes the conversion of 7 α-hydroxy-4-cholesten-3-one into 7-α,12-α-dihydroxy-4-cholesten-3-one.	ER

[1] Information was taken from www.genecards.org (accessed on 25 February 2026); Abbreviations used: ER, endoplasmic reticulum; Mit, mitochondria; N.D., not described.

We analyzed the expression of these 35 *CYP* genes in 370 cases of HCC and correlated them with the overall survival times of the patients. For six *CYP* genes (*CYP3A5*, *CYP3A43*, *CYP7A1*, *CYP19A1*, *CYP26B1*, and *CYP27A1*), we found using Kaplan–Meier statistics that high gene expression was associated with survival time ($p < 0.05$; FDR $\leq 5\%$). Among these genes, high expression of *CYP19A1* and *CYP26B1* was linked to shorter survival times, while high expression of the other four genes was associated with longer survival times (Figure 1). As an additional conservative sensitivity check, a Bonferroni-corrected threshold was calculated for the 35 tested *CYP* genes ($p_{\text{Bonferroni}} = 0.05/35 = 0.00143$) [32]. A comparison of this threshold with the *p*-values reported in Figure 1 showed that *CYP3A5*, *CYP7A1*, *CYP19A1*, and *CYP27A1* remained significant, whereas *CYP26B1* and *CYP3A43* did not pass the Bonferroni threshold. Since the Bonferroni correction controls the family-wise error rate and is highly conservative in exploratory multi-gene screening analyses, it may reduce sensitivity for detecting potentially relevant candidate genes [32]. Therefore, Benjamini–Hochberg FDR correction was used as the primary multiple-testing criterion [27].

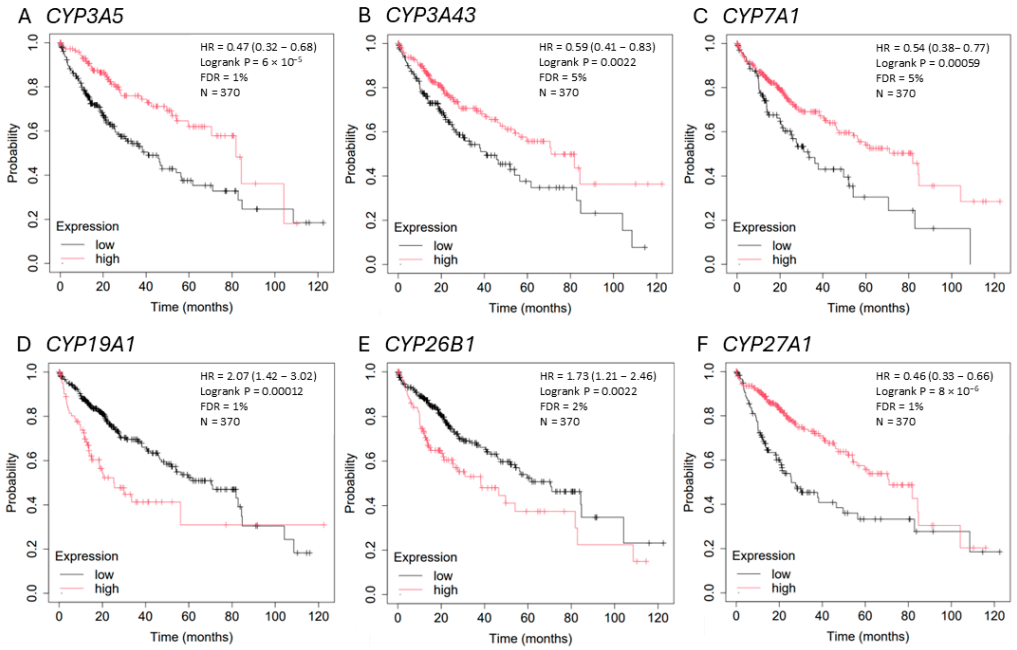


Figure 1. Prognostic relevance of CYP mRNA expression for overall survival of 370 HCC patients as determined by Kaplan–Meier statistics. (**A**) CYP3A5; (**B**) CYP3A43; (**C**) CYP7A1; (**D**) CYP19A1; (**E**) CYP26B1; (**F**) CYP27A1.

Since standard therapy for HCC generally results in unsatisfactory response rates, we were intrigued to explore conditions that could help us develop new immunotherapeutic approaches. Therefore, we first investigated the connection between *CYP* expression and the mutation rates and neo-antigen loads of tumors. These two parameters are factors that promote immunogenic cell death and the success of immunotherapeutic approaches. In fact, we found that a high mutation rate combined with all *CYP* genes except *CYP3A43* correlated with survival times (Table 2). When high *CYP* expression was combined with neoantigen load, the situation was not as clear: a high neoantigen load together with *CYP7A1*, *CYP26B1*, and *CYP27A1* led to significant differences in survival time, while a low neoantigen load and high *CYP19A1* expression were statistically significantly associated with survival time (Table 2).

Table 2. Relationship between CYP mRNA expression combined with high mutational rates or high neoantigen load, and overall survival times of HCC ($p < 0.05$ and FDR < 5%).

Gene	Number	Hazard Ratio	Log Rank (*p*)	FDR	Relationship
High mutation rates					
CYP3A5	180	0.36 (0.2–0.62)	0.00016	1%	high expression—long survival
CYP7A1	180	0.35 (0.21–0.61)	8.1×10^{-5}	1%	high expression—long survival
CYP19A1	180	2.71 (1.6–4.61)	0.00013	1%	high expression—short survival
CYP26B1	180	2.41 (1.47–3.97)	0.00035	1%	high expression—short survival
CYP27A1	180	0.37 (0.23–0.61)	4.6×10^{-5}	1%	high expression—long survival
High neoantigen loads					
CYP7A1	246	0.41 (0.26–0.63)	2.4×10^{-5}	1%	high expression—long survival
CYP26B1	246	1.93 (1.26–2.97)	0.0022	1%	high expression—short survival
CYP27A1	236	0.46 (0.3–0.71)	3×10^{-4}	3%	high expression—long survival
Low neoantigen loads					
CYP19A1	104	2.61 (1.25–5.45)	3.9×10^{-5}	3%	high expression—short survival

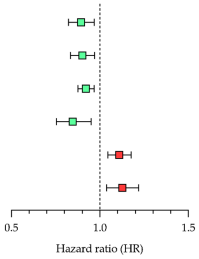
3.2. Cox Regression Analyses

To further evaluate the survival associations identified in the Kaplan–Meier analysis, we performed univariable and multivariable Cox regression analyses ($n = 325$) (Table 3). The univariable model indicates that higher expression of *CYP3A5*, *CYP3A43*, *CYP7A1*, and *CYP27A1* was associated with improved OS. In contrast, higher expression of *CYP19A1*

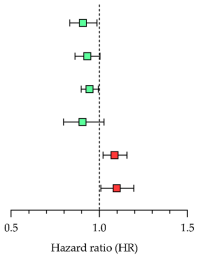
and *CYP26B1* was associated with worse OS. All six *CYP* genes were statistically significant ($p < 0.01$) and consistent with the preceding Kaplan–Meier results.

Table 3. Results and Forest plots of univariable and multivariable Cox regression analyses for overall survival in TCGA-LIHC, based on 325 evaluable cases. (**A**) Univariable Cox regression results for the six prognostic *CYP* genes. (**B**) Multivariable Cox regression results adjusted for age, sex, pathological stage, and histological grade. Hazard ratios (HR) below 1 indicate improved OS with higher gene expression, while HR above 1 indicate worse OS. In the forest plots, green squares indicate HR point estimates below 1, while red squares indicate HR point estimates above 1. Full results of the multivariable model are provided in Supplementary Table S1.

(**A**)

Gene	Univariable HR (95% CI)	*p*-Value	Forest Plot
CYP3A5	0.893 (0.823–0.969)	0.007	
CYP3A43	0.900 (0.835–0.970)	0.006	
CYP7A1	0.921 (0.877–0.967)	<0.001	
CYP27A1	0.847 (0.755–0.951)	0.005	
CYP19A1	1.109 (1.045–1.176)	<0.001	
CYP26B1	1.126 (1.039–1.220)	0.004	

(**B**)

Gene	Multivariable HR (95% CI)	*p*-Value	Forest Plot
CYP3A5	0.907 (0.833–0.987)	0.024	
CYP3A43	0.931 (0.862–1.005)	0.069	
CYP7A1	0.945 (0.897–0.995)	0.032	
CYP27A1	0.905 (0.797–1.026)	0.120	
CYP19A1	1.087 (1.021–1.157)	0.009	
CYP26B1	1.098 (1.009–1.195)	0.031	

In the multivariable model, age, sex, pathological stage, and histological grade were additionally adjusted (Table 3B). The overall pattern remained partly preserved. Higher expression of *CYP3A5* (HR 0.907; $p = 0.024$) and *CYP7A1* (HR 0.945; $p = 0.032$) remain associated with improved OS. Conversely, higher expression of *CYP19A1* (HR 1.087; $p = 0.009$) and *CYP26B1* (HR 1.098; $p = 0.031$) remained unfavorable for OS. For *CYP3A43*, the multivariable model showed borderline significance ($p = 0.069$), whereas *CYP27A1* was no longer significant ($p = 0.120$). Full multivariable Cox regression results are provided in Supplementary Table S1.

In an additional sensitivity analysis restricted to cases with available Ishak fibrosis score data ($n = 191$), *CYP19A1* (HR 1.151; 95% CI 1.038–1.275; $p = 0.008$) remained significantly associated with worse OS. The complete results are shown in Supplementary Table S2.

3.3. Survival Analysis Using Kaplan–Meier for CYP Expression and Mutational Status

In a further exploration analysis, the correlation between *CYP* mRNA expression and *TP53* and *CTNNB1* mutation status was examined. First, the mutation status alone was analyzed via Kaplan–Meier survival curves. Neither *TP53* nor *CTNNB1* mutation status was significantly associated with OS in the tested data set ($p = 0.313$ and $p = 0.629$, respectively).

Next, *CYP* expression status was combined with the mutation status of each gene. Overall, 12 *CYP*/mutation status combinations were analyzed. Nine of these combinations showed significant differences in OS, whereas the combinations *CYP26B1*/*TP53*, *CYP26B1*/*CTNNB1*, and *CYP27A1*/*TP53* were not significant with $p > 0.05$ (Tables 4 and 5).

Table 4. Data of Kaplan–Meier analysis in HCC patients grouped by *CYP* mRNA expression and *TP53* mutation status. Patients were divided into four groups based on low (↓) or high (↑) *CYP* mRNA expression and wild-type (WT) or mutated *TP53* status (mut). Mean OS is shown in months. Groups were compared using the log-rank test.

CYP	*CYP* ↓ *TP53*_WT		*CYP* ↑ *TP53*_WT		*CYP* ↓ *TP53*_Mut		*CYP* ↑ *TP53*_Mut		Log-Rank *p*
	No. of Patients	Mean OS (Months)	No. of Patients	Mean OS (Months)	No. of Patients	Mean OS (Months)	No. of Patients	Mean OS (Months)	
CYP3A5	114	59	120	73	48	46	43	61	0.040
CYP3A43	108	59	126	74	54	43	37	68	0.002
CYP7A1	117	57	117	73	45	45	46	59	0.016
CYP19A1	133	68	101	62	29	64	62	45	0.031
CYP26B1	124	69	110	62	38	58	53	46	0.079
CYP27A1	102	61	132	70	60	48	31	60	0.066

Table 5. Data of Kaplan–Meier analysis in HCC patients grouped by *CYP* mRNA expression and *CTNNB1* mutation status. Patients were divided into four groups based on low (↓) or high (↑) *CYP* mRNA expression and wild-type (WT) or mutated *CTNNB1* status (mut). Mean OS is shown in months. Groups were compared using the log-rank test.

CYP	*CYP* ↓ *CTNNB1*_WT		*CYP* ↑ *CTNNB1*_WT		*CYP* ↓ *CTNNB1*_Mut		*CYP* ↑ *CTNNB1*_Mut		Log-Rank *p*
	No. of Patients	Mean OS (Months)	No. of Patients	Mean OS (Months)	No. of Patients	Mean OS (Months)	No. of Patients	Mean OS (Months)	
CYP3A5	121	57	117	73	41	54	46	56	0.029
CYP3A43	128	53	110	80	34	47	53	57	0.007
CYP7A1	125	56	113	74	37	41	50	57	0.030
CYP19A1	102	68	136	64	60	65	27	34	0.023
CYP26B1	105	71	133	59	57	58	30	40	0.163
CYP27A1	141	60	97	72	21	43	66	60	0.041

The observed patterns were largely consistent with the survival trends described above for the individual *CYPs*. For *CYP3A5*, *CYP3A43*, *CYP7A1*, and *CYP27A1*, a higher expression was, in general, associated with a longer mean of survival within *TP53*- or *CTNNB1*-defined subgroups. This was most pronounced for *CYP3A43* in combination with *TP53* mutations ($p = 0.002$; Figure 2A and Table 4). In contrast, *CYP19A1* and *CYP26B1* showed the opposite trend, with higher expression being associated with shorter means of OS, particularly in mutation-positive subgroups. This trend was especially pronounced for *CYP19A* in combination with *CTNNB1* mutation status ($p = 0.023$; Figure 2A and Table 5). Overall, these findings suggest that the relationship between *CYP* mRNA expression and OS may be influenced, at least in part, by the mutational context of the tumor.

3.4. CYP Expression and Tumor Immune Cell Infiltration

Then, we investigated the connection between *CYP* expression and immune cell infiltration. We took statistically significant results ($p < 0.05$; FDR $\leq 5\%$) of the six selected *CYP* genes combined with 11 different immune cell types and plotted them as a matrix. We assigned a value of -1 if the immune cell counts were decreased and a value of 1 if the cell counts were increased. If no correlation was found, we assigned a value of 0. In cases where both enriched and decreased immune cell counts correlated with survival times, no value was assigned, as we assumed no specific effects of the tumor infiltration on patient survival. Similarly, we also included the results of high or low mutation rates and neo-antigen loads.

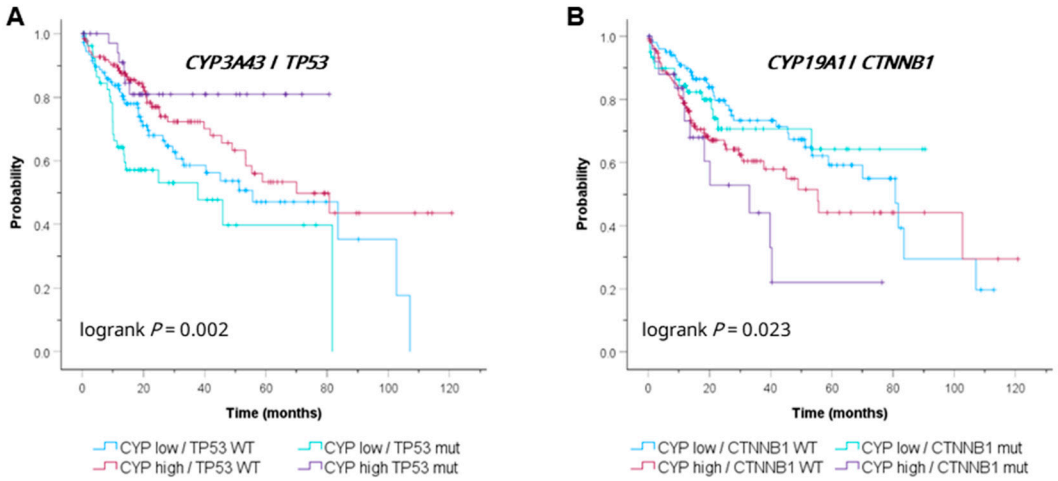


Figure 2. Kaplan–Meier analysis in HCC patients grouped by *CYP* expression and mutation status. Patients were divided into four groups based on low or high *CYP* mRNA expression and wild-type (WT) or mutated *TP53/CTNNB1* status (mut). (**A**) *CYP3A43* expression in combination with *TP53* mutation status. (**B**) *CYP19A1* expression in combination with *CTNNB1* mutation status.

This matrix was then subjected to hierarchical cluster analysis. Figure 3A shows the correlation of high *CYP* expression plus immune cell infiltration for shorter survival times, while Figure 3B shows the correlation for longer survival times. In both cluster image maps, two clusters appeared that separated the *CYP* genes from each other.

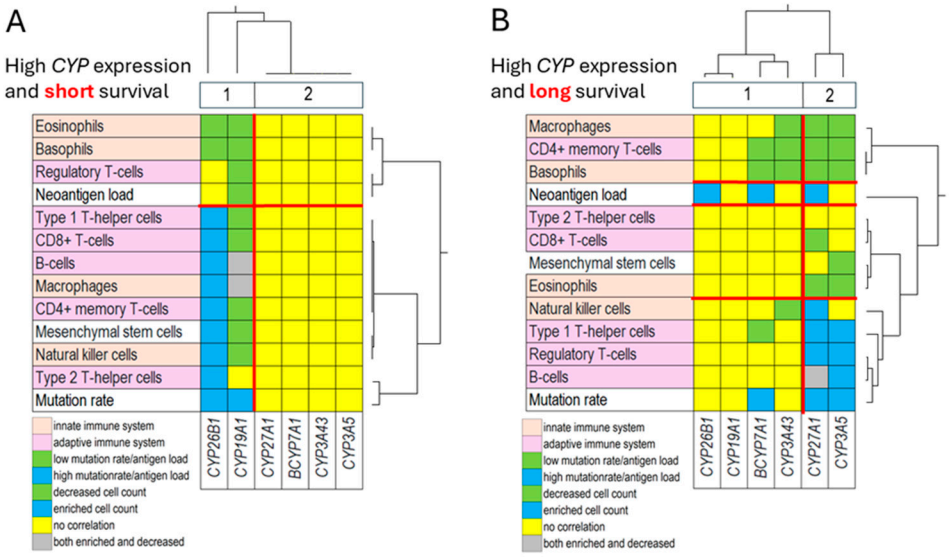


Figure 3. Hierarchical cluster analysis of Kaplan–Meier overall survival analyses of *CYP* mRNA expression combined with DNA mutation rates, neoantigen loads, and 11 immune cell types of the innate and adaptive immune system ($p < 0.05$; FDR $\leq$ 5%). (**A**) shows the cluster analysis related to short survival and (**B**) with long survival.

In Figure 3A, *CYP26B1* and *CYP19A1*, combined with the infiltration of immune cells from the innate and adaptive immune systems, clustered together in Cluster 1, indicating that these *CYP*/immune cell combinations were relevant for the patients' survival. On the other hand, the immune cell infiltration and expression of the other four *CYP* genes did not significantly affect survival times (Cluster 2). Interestingly, high mutation and neo-antigen load clustered along with the immune cell counts, and both parameters were also found in Cluster 1.

In Figure 3B, a similar analysis was conducted for patients with longer survival times. Cluster 1 consisted of a mixed type with most, but not all, combinations of *CYP*/immune cell counts being insignificant. Specifically, the genes *CYP26B1*, *CYP19A1*, *CYP7A1*, and *CYP3A4* were grouped in this cluster. In Cluster 2, the majority of *CYP*/immune cell count pairs showed a significant correlation with longer survival, particularly for the genes *CYP27A1* and *CYP3A5*. High mutation rates were clustered along with immune cell counts in Cluster 2, while high neo-antigen loads were found in both clusters.

Additional correlation analysis between the expression of the six CYPs and functional signatures of immune activation or exhaustion was performed. Correlation analysis showed an association between the expression of the selected CYPs and the immune genes. *CYP19A1* and *CYP26B* (associated with a worse prognosis) exhibited positive correlations with immune exhaustion markers, including PDCD1, *CTLA4*, and *HAVCR2*, as presented in cluster AD (Figure 4) and negative correlations with activation markers such as *GZMB*, *PRF1*, and *IFNG* in cluster BD (Figure 4). The other CYPs (*CYP3A5*, *CYP7A1*, *CYP3A43*, and *CYP27A1*) showed the opposite pattern, displaying negative associations with exhaustion markers in cluster AC (Figure 4) and positive correlations with immune activation genes in cluster BC (Figure 4).

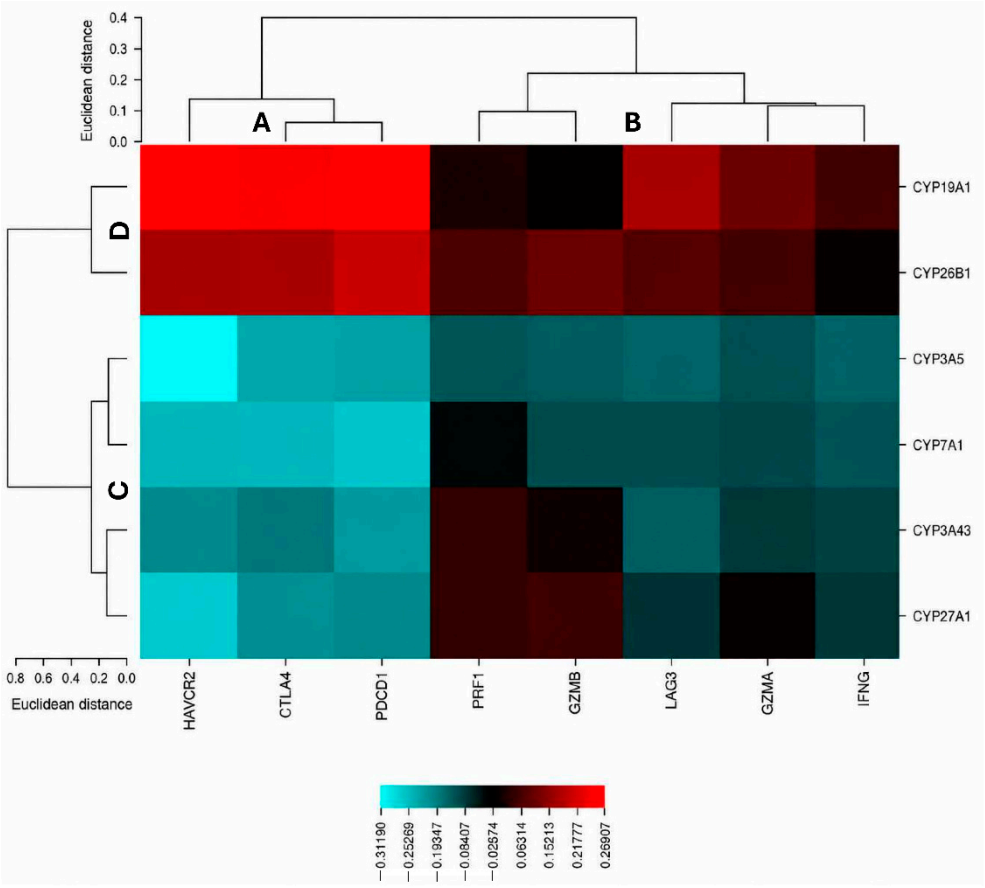


Figure 4. Correlation between CYP expression and functional signatures of immune activation or exhaustion. Spearman correlation coefficient was carried out using GraphPad Prism between the *CYP* genes (rows) and the immune activation/exhaustion genes (columns) for TGCA tumor samples. The red color represents the positive correlation, while the blue color indicates the negative correlation. Cluster A corresponds to inhibitory/exhaustion-associated immune markers (HAVCR2, CTLA4, PDCD1), cluster B presents cytotoxic/effector-associated immune markers (PRF1, GZMB, LAG3, GZMA, IFNG), cluster C and D represent the *CYP* genes.

Hierarchical clustering further supported the separation of CYPs into two distinct CYP groups associated with immunosuppressive versus immune-activation states. These results revealed that *CYP* expression patterns are directly linked to the functional status of the tumor immune microenvironment.

3.5. CYP mRNA Expression Levels in HCC Versus Normal Liver Tissue

It was interesting to compare *CYP* expression in HCC with that in normal liver tissue. *CYP3A5*, *CYP7A1*, and *CYP19A1* were expressed at higher levels in tumors than in normal liver tissue, although the overall expression of *CYP19A1* was lower in both tumor and normal liver samples compared to the other two *CYP* genes. In contrast, *CYP3A43*, *CYP27A1*, and *CYP26B1* were expressed at higher levels in normal liver biopsies than in tumors, although *CYP26B1* was also lower overall in normal liver and tumor samples (Figure 5).

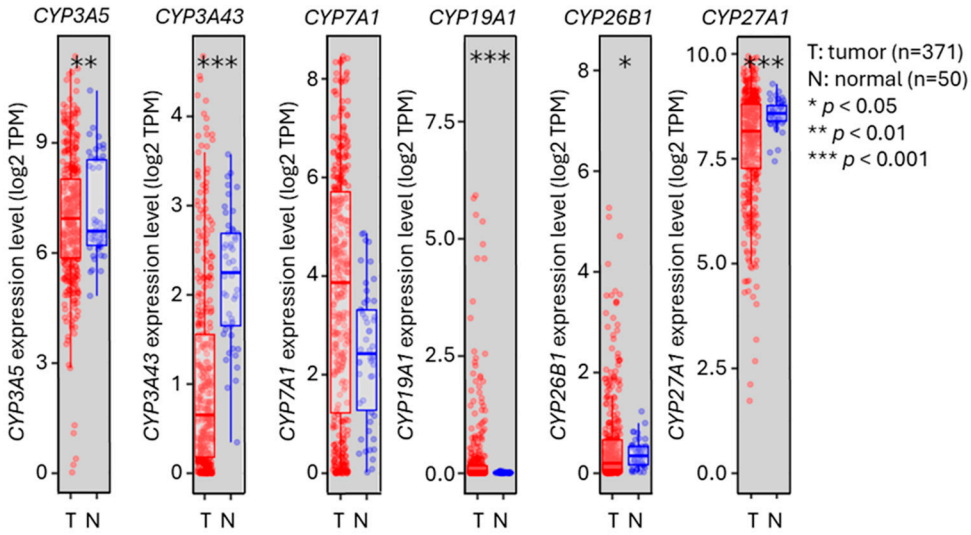


Figure 5. CYP mRNA expression in HCC compared to normal liver tissue. Red indicates HCC samples; blue indicates normal liver tissue.

4. Discussion

In this study, a total of 35 *CYP* genes were analyzed for their prognostic relevance to the overall survival of HCC patients. The mRNA expression of six genes was significantly associated with survival time. The expression of *CYP3A5*, *CYP3A43*, *CYP7A1*, and *CYP27A1* correlated with longer survival, while the expression of *CYP19A1* and *CYP26B1* was associated with shorter survival. These results suggest that there are two different functional groups of *CYP* genes with prognostic potential. The first group prolongs survival because these genes contribute to liver-specific physiology and are associated with lower tumor aggressiveness. The liver is rich in immune cells and is the main organ of lipid and bile acid metabolism in the body, which stimulates immune functions [33,34]. Due to the constant interaction between the intestine and liver (gut-liver axis), the liver is exposed to high antigen concentrations [35]. The liver is therefore a unique metabolic-immunological organ in which metabolic signaling pathways can be particularly relevant for tumors in terms of prognosis. *CYP7A1* is involved in bile acid metabolism, while the *CYP27A1*, *CYP3A5*, and *CYP3A43* enzymes are involved in lipid and steroid metabolism [36–42]. A metabolic influence on tumor immunity, which has a favorable effect on survival time, is therefore evident. The second group contains genes that are known to amplify proliferative signals, such as through estrogen synthesis (*CYP19A1*) and retinoic acid metabolism (*CYP26B1*) [43,44]. This can cause liver tumors to become more aggressive and grow faster.

A major limitation of this study is its reliance on The Cancer Genome Atlas cohort, which is exclusively composed of surgically resected, treatment-naive tumor samples and thus depicts a population with earlier-stage disease [45]. In clinical practice, most HCC patients are not candidates for surgery and are instead treated with locoregional therapies such as TACE (for intermediate stage disease), or systemic immunotherapies (for advanced stage disease) [46]. These groups are not represented in TCGA [45] and may have significantly different clinical and biological characteristics than *CYP* expression profiles, which may be changed by the severity of the disease [47], the immune microenvironment, which is influenced by the disease stage [48], and tumor burden and liver function, which systematically differ between resectable and non-resectable patients [46,49]. This restricts the generalizability of our results. Consequently, validation in independent cohorts, including HCC patients receiving systemic and locoregional therapy, is essential.

Given that *CYP* expression may be influenced by the aforementioned factors, we conducted univariable and multivariable Cox regression analyses. Notably, Cox regression analyses corroborated *CYP3A5*, *CYP7A1*, *CYP19A1*, and *CYP26B1* as independent prognostic factors after age, sex, pathological stage, and histological grade were adjusted. However, *CYP3A43* and *CYP27A1* lost significance in the multivariable model. The prognostic value of *CYP19A1* was also confirmed after fibrosis adjustment, though given the reduced sample size and the use of an Ishak-based surrogate rather than a uniformly documented cirrhosis variable, these findings should be interpreted as supportive sensitivity analyses rather than definitive evidence of fibrosis-independent effects.

Interestingly, we found no correlation between survival times and classic drug-metabolizing CYPs (e.g., *CYP1A2*, *CYP3A4*, *CYP2C9*, *CYP2C19*, and *CYP2D6*), which play a central role in the detoxification of xenobiotics and drug metabolism. This suggests that the breakdown of foreign substances by pharmacokinetic CYPs plays a minor role in tumor progression compared to the endogenous metabolic regulation of the tumor microenvironment, in which the metabolic signaling CYPs are involved. Our results suggest that it is not drug metabolism but hepatic lipid and steroid metabolism that are prognostically relevant for HCC.

Despite our results, previous studies revealed that the relationship between *CYP* expression and patient prognosis is likely multifactorial, reflecting not only their role in xenobiotic metabolism but also their contribution to other signaling pathways. For instance, the main function of some CYPs, such as *CYP3A4*, is to metabolize many chemotherapy drugs. Zangar et al. (2004) demonstrated that poor coupling of the P450 catalytic cycle leads to the accumulation of ROS, which affects cellular signaling pathways [50]. Another study showed the ability of the *CYP1A1*/*CYP1A2* to induce ROS formation and disrupt the redox state within cancer cells as a result of aminoflavone metabolism. Most probably, aminoflavone is converted into an electrophilic species and a hydroxylated metabolite, which elevate the ROS levels within these cells [51]. Moreover, the cytochromes also metabolize arachidonic acid and convert it to hydroxyeicosatetraenoic acids (HETEs). The 20-HETE is a pro-inflammatory mediator that produces inflammatory cytokines/chemokines in endothelial cells, including IL-8, IL-13, IL-4, and prostaglandin E_2 [52].

Another important finding was that high DNA mutation rates in combination with high expression of five of the six *CYP* genes correlated with survival time.

High mutation rates increase the likelihood of more neoantigens on the surface of tumor cells, and neoantigens are of central importance for immune recognition [53,54]. The coupling of *CYP* expression with the mutation rate may indicate the immunological activity of HCC. However, the neoantigen load alone is not sufficient as an explanation, since both high neoantigen load with high *CYP* expression (*CYP7A1*, *CYP26B1*, and *CYP27A1*) and low neoantigen load with high *CYP19A1* expression were observed. At the very least, our

results suggest complex interactions between tumor metabolism and tumor immunology and that *CYP* genes regulate this interface.

The exploratory analysis combining *CYP* expression with *TP53* and *CTNNB1* mutation status suggests that the association between *CYP* expression and overall survival may partly depend on the mutational context. Since *TP53* and *CTNNB1* alone were not significant, but the combined *CYP*/mutation groups showed additional survival differences, *CYP* expression might add prognostic information beyond mutation status alone.

For this reason, in the second part of our investigation, we focused on the significance of immune cell infiltration in connection with *CYP* expression. Using hierarchical cluster analysis, we found that, in the first cluster, high expression of *CYP26B1* and *CYP19A1*, a high mutation rate, a high neoantigen burden, and strong infiltration by cells from the innate and adaptive immune systems were associated with shorter survival times. The fact that patients die earlier despite high immune cell infiltration suggests dysfunctional immune activation, possibly due to infiltrating immune cells being functionally exhausted.

On the other hand, in the second cluster analysis, *CYP27A1* and *CYP3A5* expression, immune cell infiltration, and a high mutation rate correlated with longer survival in cluster 2. Not only was there high immune cell infiltration but also functioning immune recognition. However, a high neoantigen load was observed in both clusters of the second cluster analysis, indicating relatively unstable prognostic value.

The question arises as to how *CYP* genes can causally influence immune status. The *CYP* genes we have identified regulate the metabolism of lipids, steroids, bile acids, and retinoids. These metabolites influence immune cell function, tumor differentiation, and inflammation in the tumor microenvironment. Therefore, a causal relationship between *CYP* expression and tumor immunity is plausible.

CYP19A1 has aromatase activity and converts androgens into estrogens. The *CYP19A1*-expression and *CYP19A1*-mediated aromatase activity are increased in progressive HCC [55,56]. Estrogens modulate T-cell activation, Treg differentiation, macrophage polarization, and control cytokine release [57–60]. These functions can promote an immunosuppressive tumor microenvironment.

CYP26B1 metabolizes retinoic acid, which regulates T cell differentiation, dendritic cell maturation, and cytotoxic CD8+ T cell functions [61–63]. Therefore, low levels of retinoic acid can lead to weak antitumor immune responses.

CYP27A1 links cholesterol to bile acid and oxysterol metabolism. *CYP7A1* is a key enzyme in classical bile acid synthesis [64,65]. Bile acids and oxysterols affect immune cell migration, regulate macrophage polarization, affect natural killer cells, and modulate inflammatory FXR and TGR5-coupled signal transduction pathways [66–72]. Altered bile acid profiles exert immunomodulatory effects on the tumor microenvironment.

CYP3A5 and *CYP3A43* have been less well studied as yet but are also involved in steroid and lipid metabolism and thus influence the immune response [40,73]. They may additionally reflect the differentiation status of HCC. Therefore, the association of high *CYP* expression levels could explain the better survival rates in less differentiated and less aggressive tumors.

There are initial indications that *CYP* genes function as metabolic immunomodulators, not only for HCC but also for other tumor types. In breast cancer, *CYP19A1* has been shown to produce estrogen as aromatase in tumors, which stimulates immunomodulatory effects [74]. In endometrial carcinomas, *CYP19A1* was associated with hormonal activity and tumor development [75]. In prostate carcinoma, *CYP19A1* was also found to be prognostically relevant [76,77]. Furthermore, androgen levels and androgen deprivation therapy influence the immune system in prostate carcinoma [78,79]. Thus, the concept of *CYP* gene-driven metabolic immunomodulation seems to be valid not only for

HCC but also for other tumor types as a new emerging concept. However, it still needs further establishment.

The comparison of *CYP* expression in normal liver and HCC revealed interesting changes. Some CYPs were expressed at higher levels in tumors than in normal tissue (*CYP3A5*, *CYP7A1*, and *CYP19A1*), while others showed the opposite pattern (*CYP3A43*, *CYP27A1*, and *CYP26B1*). *CYP19A1* and *CYP26B1* were expressed at much lower levels overall in both normal liver and tumor samples than the other four *CYP* genes. The tumor-specific up- and down-regulation of *CYP* genes reflects how HCC alters its metabolic regulation and adapts to the selection pressure during hepatocarcinogenesis and progression. This ultimately leads to the selection of aggressive cell populations and evasion of the immune response. Nevertheless, it should be noted that the differential expression of the *CYP* genes does not always reflect the tumor immunity. Therefore, functional studies in vitro and in animal models should be established.

Next, we were intrigued by the potential practical implications of the connection between *CYP* genes and immune cell infiltration for the clinical management of HCC. Standard therapy is often effective, but there is a need for the development of new diagnostic and therapeutic strategies. Despite the significant chemoresistance of HCC, immunotherapeutic approaches have shown some success [80]. Liver tumors usually arise from inflammatory liver conditions such as hepatitis infections, fibrosis, steatosis, steatohepatitis, or cirrhosis, leading to the activation of many pre-primed T cells by checkpoint inhibitors. Treatment with checkpoint inhibitors prevents T cell exhaustion, maintaining the systemic effect of the immune response against the tumor. This effect is further enhanced by neoangiogenesis inhibitors such as bevacizumab [11,81]. Normalizing tumor angiogenesis promotes T cell infiltration. However, immunotherapy alone cannot completely eradicate the disease, and patient survival rates are still below optimal levels. This raises the question of how therapeutic options can be further optimized.

Signatures from *CYP* expression could potentially serve as predictive biomarkers for the response to immunotherapies. By combining signatures from *CYP* expression, mutation rate, and immune status, patients could be stratified to select tumors with an immune-active ("hot") tumor microenvironment for appropriate immunotherapies.

The combined analyses of *CYP* expression, mutation rate, and immune status not only suggest the potential benefits of immunotherapy but also indicate that combination therapy with classic anticancer drugs may result in additive or synergistic effects. Doxorubicin and cisplatin, commonly used for TACE, induce DNA strand breaks, leading to increased DNA mutation rates and neoantigen generation. This can enhance the body's immune response to HCC, ultimately improving patient survival times [82]. This process is known as immunogenic cell death [83–85]. Given that metabolic CYP enzymes influence immune cell function, combining TACE with immunotherapies such as immune checkpoint inhibitors (ICIs) could result in improved treatment outcomes. Although the current investigation did not evaluate the relationship between CYP expression and responsiveness to combination therapy (TACE and ICIs), emerging studies support the biological validity of this hypothesis. The effectiveness of chemotherapeutic drugs used in TACE can be affected by CYP enzymes, especially CYP3A4, a crucial enzyme for hepatic drug metabolism, which has been demonstrated to influence chemoresistance to doxorubicin used in TACE, with its activity modulated by tumor microenvironmental elements like tissue stiffness and hypoxia, and thus contributes to interpatient variation in treatment response [86].

Additionally, molecular classification of HCC subtypes, based on zonated metabolic properties, has revealed a Wnt/β-catenin-high subtype distinguished by increased CYP3A4 expression and an immune-desert phenotype marked by low expression of immune checkpoint molecules, emphasizing the interplay of CYP-related metabolic heterogeneity and

the immune microenvironment [87]. Taking into consideration that only a fraction of HCC patients respond to ICIs and that established prognostic biomarkers are still lacking in clinical practice [88], integrating *CYP* expression into patient stratification procedures could help distinguish those who presumably will benefit from the combination of TACE and ICIs. This hypothesis should be further investigated in future research studies and clinical cohorts. Besides TACE, *CYP* expression profiles may also influence the selection of systemic therapy. As sorafenib and regorafenib are mainly metabolized by *CYP3A4/5* and their oxidative metabolism is significantly decreased in HCC tumor tissues, the prognostic significance of *CYP3A5* expression reported in this study may guide dose individualization of these targeted cancer agents [89,90].

Furthermore, other drug combinations are conceivable. In tumors with high *CYP19A1* expression, aromatase inhibition (e.g., with letrozole) could potentially alter the immunosuppressive tumor microenvironment and enhance the effectiveness of immune checkpoint inhibitors [91]. The regulation of bile acid and oxysterol levels by *CYP7A1* and *CYP27A1* could also be utilized for immunotherapy, as bile acids can enhance the immunogenicity of tumors [92,93]. *CYP26B1* metabolizes retinoic acid, and the degradation of retinoic acid is linked to HCC development [94]. Retinoic acid metabolism blocking agents (RAMBAs) inhibit the breakdown of endogenous retinoic acid by *CYP26B1* (and other *CYP26* isoforms), leading to increased retinoic acid levels and resulting in anti-proliferative and differentiation-promoting effects in tumors [95]. Additionally, the immunomodulatory properties of retinoic acid have a beneficial impact on the immune response [63,96], including in HCC [97]. However, since *CYP19A1* and *CYP26B1* were only minimally expressed in our analyses, these combination strategies may be less effective compared to TACE combined with checkpoint inhibitors. Further investigation is needed in the future.

5. Conclusions

In conclusion, we found that six out of 35 *CYP* genes significantly correlated with the survival times of HCC patients (*CYP3A5*, *CYP3A43*, *CYP7A1*, *CYP19A1*, *CYP26B1*, and *CYP27A1*). These CYPs are involved in metabolic regulation rather than classical drug metabolism. Combined signatures consisting of *CYP* expression, mutational rates, and immune cell infiltration into tumors enhance the prognostic value for patient survival. This suggests that CYPs may create a tumor-specific metabolic microenvironment that modulates immune functions. These combined signatures could be utilized for patient stratification to personalize tumor treatment and for the development of novel combination treatments to optimize outcomes (e.g., TACE plus immune checkpoint inhibitors).

Supplementary Materials: The following supporting information can be downloaded at: https://www.mdpi.com/article/10.3390/livers6030050/s1, Table S1: Multivariable Cox regression models for overall survival in TCGA-LIHC (n = 325). All models were adjusted for age, sex, pathological stage, and histological grade. Sex was coded as male versus female, pathological stage as stage III/IV versus stage I/II, and histological grade as G3/G4 versus G1/G2.; Table S2: Multivariable Cox regression models for overall survival in TCGA-LIHC, including an Ishak fibrosis/cirrhosis surrogate (n = 191). All models were adjusted for age, sex, pathological stage, and histological grade. Sex was coded as male versus female, pathological stage as stage III/IV versus stage I/II, histological grade as G3/G4 versus G1/G2, and cirrhosis status as Ishak 0–4 versus Ishak 5–6.

Author Contributions: Conceptualization, T.E.; validation, M.D., E.O., R.W., T.E. and J.C.B.; investigation, M.D. and A.G.; resources, T.E., R.W. and J.C.B.; data curation, M.D. and A.G.; writing—original draft preparation, J.C.B.; writing—review and editing, M.D., T.E. and R.W.; visualization, M.D.; supervision, T.E.; project administration, E.O. All authors have read and agreed to the published version of the manuscript.

Funding: This research received no external funding. Ednah Ooko is funded by the NIH Intramural Research Program of the National Institute of Health (NIH), National Cancer Institute (NCI), and Center for Cancer Research, Bethesda, MD, USA.

Institutional Review Board Statement: Ethical review and approval were not required because this study was based solely on data extracted from previously published mRNA expression data deposited in the TCGA and KMPlot databases and did not involve direct human participation or identifiable personal data.

Informed Consent Statement: Informed consent was not required because the study used only anonymized, publicly available data from previously published mRNA expression data deposited in the TCGA and KMPlot databases.

Data Availability Statement: The original contributions presented in this study are included in the article/Supplementary Material. Further inquiries can be directed to the corresponding author.

Conflicts of Interest: The authors declare no conflicts of interest.

Abbreviations

The following abbreviations are used in this manuscript:

CD	Cluster of differentiation
CYP	Cytochrome P450 monooxygenase
FDR	False discovery rate
HBV	Chronic hepatitis B virus
HCC	Hepatocellular carcinoma
HCV	Hepatitis C virus
KM	Kaplan–Meier
MWA	Microwave ablation
NAFLD	Non-alcoholic fatty liver disease
NASH	Non-alcoholic steatohepatitis
PD-L1	Programmed cell death1 ligand 1
RFA	Radiofrequency ablation
ROS	Reactive oxygen species
SIRT	Selective internal radiotherapy
TACE	Transarterial chemoembolization
TARE	Transarterial radioembolization
TCGA	The Cancer Genome Atlas
VEGF	Vascular endothelial growth factor

References

1. Lafaro, K.J.; Demirjian, A.N.; Pawlik, T.M. Epidemiology of hepatocellular carcinoma. *Surg. Oncol. Clin.* **2015**, *24*, 1–17. [CrossRef] [PubMed]
2. Seven, İ.; Bayram, D.; Arslan, H.; Köş, F.T.; Gümüşlü, K.; Aktürk Esen, S.; Şahin, M.; Şendur, M.A.N.; Uncu, D. Predicting hepatocellular carcinoma survival with artificial intelligence. *Sci. Rep.* **2025**, *15*, 6226. [CrossRef] [PubMed]
3. Vogel, A.; Meyer, T.; Sapisochin, G.; Salem, R. Saborowski A Hepatocellular carcinoma. *Lancet* **2022**, *400*, 1345. [CrossRef]
4. Chen, L.; Wang, Y.; Li, S.; Lu, S.; Luo, Y.; Ning, Y.; Chen, J.; Zhou, S. Metabolic syndrome-related gene signature for prognosis and immune microenvironment prediction in hepatocellular carcinoma. *Sci. Rep.* **2025**, *15*, 39048. [CrossRef]
5. Tang, R.; Liu, H.; Yuan, Y.; Xie, K.; Xu, P.; Liu, X.; Wen, J. Genetic factors associated with risk of metabolic syndrome and hepatocellular carcinoma. *Oncotarget* **2017**, *8*, 35403–35411. [CrossRef]
6. Cornellà, H.; Alsinet, C.; Villanueva, A. Molecular Pathogenesis of Hepatocellular Carcinoma. *Alcohol. Clin. Exp. Res.* **2011**, *35*, 821–825. [CrossRef] [PubMed]
7. Sakamoto, M.; Effendi, K.; Masugi, Y. Molecular diagnosis of multistage hepatocarcinogenesis. *Jpn. J. Clin. Oncol.* **2010**, *40*, 891–896. [CrossRef]
8. Wu, M.-Y.; Yiang, G.-T.; Cheng, P.-W.; Chu, P.-Y.; Li, C.-J. Molecular targets in hepatocarcinogenesis and implications for therapy. *J. Clin. Med.* **2018**, *7*, 213. [CrossRef]

9. de Alcântara, J.; Götz, G. Transarterial Radioembolization with Yttrium-90 and SIRT Versus Conventional Transarterial Chemoembolization for Hepatocellular Carcinoma: A Systematic Review and Meta-analysis. *Acad. Radiol.* **2025**, *32*, 6739–6750. [CrossRef]
10. Zane, K.E.; Makary, M.S. Locoregional Therapies for Hepatocellular Carcinoma with Portal Vein Tumor Thrombosis. *Cancers* **2021**, *13*, 5430. [CrossRef]
11. Finn, R.S.; Qin, S.; Ikeda, M.; Galle, P.R.; Ducreux, M.; Kim, T.-Y.; Kudo, M.; Breder, V.; Merle, P.; Kaseb, A.O.; et al. Atezolizumab plus bevacizumab in unresectable hepatocellular carcinoma. *N. Engl. J. Med.* **2020**, *382*, 1894–1905. [CrossRef] [PubMed]
12. Dai, S.; Chen, Y.; Cai, W.; Dong, S.; Zhao, J.; Chen, L.; Cheng, C.S. Combination immunotherapy in hepatocellular carcinoma: Synergies among immune checkpoints, TKIs, and chemotherapy. *J. Hematol. Oncol.* **2025**, *18*, 85. [CrossRef] [PubMed]
13. Forner, A.; Reig, M.; Bruix, J. Hepatocellular carcinoma. *Lancet* **2018**, *391*, 1301–1314. [CrossRef]
14. Ikeda, M.; Morizane, C.; Ueno, M.; Okusaka, T.; Ishii, H.; Furuse, J. Chemotherapy for hepatocellular carcinoma: Current status and future perspectives. *Jpn. J. Clin. Oncol.* **2018**, *48*, 103–114. [CrossRef]
15. Garg, A.D.; More, S.; Rufo, N.; Mece, O.; Sassano, M.L.; Agostinis, P.; Zitvogel, L.; Kroemer, G.; Galluzzi, L. Trial watch: Immunogenic cell death induction by anticancer chemotherapeutics. *Oncoimmunology* **2017**, *6*, e1386829. [CrossRef]
16. Pinato, D.J.; Murray, S.M.; Forner, A.; Kaneko, T.; Fessas, P.; Toniutto, P.; Mínguez, B.; Cacciato, V.; Avellini, C.; Diaz, A.; et al. Trans-arterial chemoembolization as a loco-regional inducer of immunogenic cell death in hepatocellular carcinoma: Implications for immunotherapy. *J. Immunother. Cancer* **2021**, *9*, e003311. [CrossRef]
17. Zhang, Y.; Yang, J.; Xie, S.; Chen, H.; Zhong, J.; Lin, X.; Yu, Z.; Xia, J. A novel prognostic signature based on immunogenic cell death score predicts outcomes and response to transcatheter arterial chemoembolization and immunotherapy in hepatocellular carcinoma. *J. Cancer Res. Clin. Oncol.* **2023**, *149*, 11411–11429. [CrossRef]
18. Zhu, H.; Shan, Y.; Ge, K.; Lu, J.; Kong, W.; Jia, C. Oxaliplatin induces immunogenic cell death in hepatocellular carcinoma cells and synergizes with immune checkpoint blockade therapy. *Cell. Oncol.* **2020**, *43*, 1203–1214. [CrossRef]
19. Liu, Q.Q.; Wang, X.X.; Ji, H.; Dou, Q.Y.; Zhang, H.M. The efficacy and safety of PD-1 inhibitor combined with TACE in the first-line treatment of unresectable hepatocellular carcinoma. *Med. Oncol.* **2024**, *41*, 91. [CrossRef] [PubMed]
20. Hao, L.; Li, S.; Ye, F.; Wang, H.; Zhong, Y.; Zhang, X.; Hu, X.; Huang, X. The current status and future of targeted-immune combination for hepatocellular carcinoma. *Front. Immunol.* **2024**, *15*, 1418965. [CrossRef]
21. Abu-Bakar, A.; Tan, B.H.; Halim, H.; Ramli, S.; Pan, Y.; Ong, C.E. Cytochromes P450: Role in Carcinogenesis and Relevance to Cancers. *Curr. Drug Metab.* **2022**, *23*, 355–373. [CrossRef] [PubMed]
22. Bagdasaryan, A.A.; Chubarev, V.N.; Smolyarchuk, E.A.; Drozdov, V.N.; Krasnyuk, I.I.; Liu, J.; Fan, R.; Tse, E.; Shikh, E.V.; Sukocheva, O.A. Pharmacogenetics of Drug Metabolism: The Role of Gene Polymorphism in the Regulation of Doxorubicin Safety and Efficacy. *Cancers* **2022**, *14*, 5436. [CrossRef]
23. McGill, M.R.; Kaufman, Y.J.; LoBianco, F.V.; Schleiff, M.A.; Aykin-Burns, N.; Miller, G.P. The role of cytochrome P450 3A4-mediated metabolism in sorafenib and lapatinib hepatotoxicity. *Livers* **2023**, *3*, 310–321. [CrossRef]
24. Lévesque, J.F.; Day, S.H.; Jones, A.N. Protocols of in vitro protein covalent binding studies in liver. *Methods Mol. Biol.* **2011**, *691*, 283–301. [CrossRef]
25. Győrffy, B. Integrated analysis of public datasets for the discovery and validation of survival-associated genes in solid tumors. *Innovation* **2024**, *5*, 100625. [CrossRef] [PubMed]
26. Ooko, E.; Efferth, T. Identification of Prognostic Gene Signatures for Survival of Patients With Phaeochromocytoma, Paraganglioma, and Other Tumor Types. *Cancer Diagn. Progn.* **2025**, *5*, 808–832. [CrossRef]
27. Benjamini, Y.; Hochberg, Y. Controlling the False Discovery Rate: A Practical and Powerful Approach to Multiple Testing. *J. R. Stat. Soc. Ser. B (Methodol.)* **1995**, *57*, 289–300. [CrossRef]
28. Heath, A.P.; Ferretti, V.; Agrawal, S.; An, M.; Angelakos, J.C.; Arya, R.; Bajari, R.; Baqar, B.; Barnowski, J.H.B.; Burt, J.; et al. The NCI Genomic Data Commons. *Nat. Genet.* **2021**, *53*, 257–262. [CrossRef]
29. Goldman, M.J.; Craft, B.; Hastie, M.; Repečka, K.; McDade, F.; Kamath, A.; Banerjee, A.; Luo, Y.; Rogers, D.; Brooks, A.N.; et al. Visualizing and interpreting cancer genomics data via the Xena platform. *Nat. Biotechnol.* **2020**, *38*, 675–678. [CrossRef]
30. Ellrott, K.; Bailey, M.H.; Saksena, G.; Covington, K.R.; Kandoth, C.; Stewart, C.; Hess, J.; Ma, S.; Chiotti, K.E.; McLellan, M.; et al. Scalable Open Science Approach for Mutation Calling of Tumor Exomes Using Multiple Genomic Pipelines. *Cell Syst.* **2018**, *6*, 271–281.E7. [CrossRef] [PubMed]
31. Li, T.; Fu, J.; Zeng, Z.; Cohen, D.; Li, J.; Chen, Q.; Li, B.; Liu, X.S. TIMER2.0 for analysis of tumor-infiltrating immune cells. *Nucleic Acids Res.* **2020**, *48*, W509–W514. [CrossRef] [PubMed]
32. Noble, W.S. How does multiple testing correction work? *Nat. Biotechnol.* **2009**, *27*, 1135–1137. [CrossRef] [PubMed]
33. Fiorucci, S.; Marchianò, S.; Urbani, G.; Di Giorgio, C.; Distrutti, E.; Zampella, A.; Biagioli, M. Immunology of bile acids regulated receptors. *Prog. Lipid Res.* **2024**, *95*, 101291. [CrossRef]
34. Jia, W.; Li, Y.; Cheung, K.C.P.; Zheng, X. Bile acid signaling in the regulation of whole body metabolic and immunological homeostasis. *Sci. China Life Sci.* **2024**, *67*, 865–878. [CrossRef]

35. Tilg, H.; Adolph, T.E.; Trauner, M. Gut-liver axis: Pathophysiological concepts and clinical implications. *Cell Metab.* **2022**, *34*, 1700–1718. [CrossRef]
36. Cali, J.J.; Russell, D.W. Characterization of human sterol 27-hydroxylase. A mitochondrial cytochrome P-450 that catalyzes multiple oxidation reaction in bile acid biosynthesis. *J. Biol. Chem.* **1991**, *266*, 7774–7778. [CrossRef]
37. Chambers, K.F.; Day, P.E.; Aboufarrag, H.T.; Kroon, P.A. Polyphenol Effects on Cholesterol Metabolism via Bile Acid Biosynthesis, CYP7A1: A Review. *Nutrients* **2019**, *11*, 2588. [CrossRef]
38. Chiang, J.Y.L.; Ferrell, J.M. Up to date on cholesterol 7 alpha-hydroxylase (CYP7A1) in bile acid synthesis. *Liver Res.* **2020**, *4*, 47–63. [CrossRef] [PubMed]
39. Escher, G.; Krozowski, Z.; Croft, K.D.; Sviridov, D. Expression of sterol 27-hydroxylase (CYP27A1) enhances cholesterol efflux. *J. Biol. Chem.* **2003**, *278*, 11015–11019. [CrossRef]
40. Klyushova, L.S.; Perepechaeva, M.L.; Grishanova, A.Y. The Role of CYP3A in Health and Disease. *Biomedicines* **2022**, *10*, 2686. [CrossRef]
41. Niwa, T.; Murayama, N.; Imagawa, Y.; Yamazaki, H. Regioselective hydroxylation of steroid hormones by human cytochromes P450. *Drug Metab. Rev.* **2015**, *47*, 89–110. [CrossRef]
42. Pikuleva, I.A. Cholesterol-metabolizing cytochromes P450. *Drug Metab. Dispos. Biol. Fate Chem.* **2006**, *34*, 513–520. [CrossRef]
43. Lee, Y.B.; Kim, C.; Hong, J.; Kim, D. Molecular insights into CYP19A1 mutations and their role in estrogen production. *Arch. Biochem. Biophys.* **2025**, *772*, 110573. [CrossRef]
44. Topletz, A.R.; Thatcher, J.E.; Zelter, A.; Lutz, J.D.; Tay, S.; Nelson, W.L.; Isoherranen, N. Comparison of the function and expression of CYP26A1 and CYP26B1, the two retinoic acid hydroxylases. *Biochem. Pharmacol.* **2012**, *83*, 149–163. [CrossRef]
45. Ally, A.; Balasundaram, M.; Carlsen, R.; Chuah, E.; Clarke, A.; Dhalla, N.; Holt, R.A.; Jones, S.J.M.; Lee, D.; Ma, Y.; et al. Comprehensive and Integrative Genomic Characterization of Hepatocellular Carcinoma. *Cell* **2017**, *169*, 1327–1341.E23. [CrossRef]
46. Marina, R.; Forner, A.; Rimola, J. BCLC strategy for prognosis prediction and treatment recommendation: The 2022 update. *J. Hepatol.* **2021**, *19*, S0168–S8278.
47. Brown, Z.J.; Ruff, S.M.; Pawlik, T.M. The effect of liver disease on hepatic microenvironment and implications for immune therapy. *Front. Pharmacol.* **2023**, *14*, 1225821. [CrossRef]
48. Llovet, J.M.; Castet, F.; Heikenwalder, M.; Maini, M.K.; Mazzaferro, V.; Pinato, D.J.; Pikarsky, E.; Zhu, A.X.; Finn, R.S. Immunotherapies for hepatocellular carcinoma. *Nat. Rev. Clin. Oncol.* **2022**, *19*, 151–172. [CrossRef] [PubMed]
49. Kinsey, E.; Lee, H.M. Management of hepatocellular carcinoma in 2024: The multidisciplinary paradigm in an evolving treatment landscape. *Cancers* **2024**, *16*, 666. [CrossRef] [PubMed]
50. Zangar, R.C.; Davydov, D.R.; Verma, S. Mechanisms that regulate production of reactive oxygen species by cytochrome P450. *Toxicol. Appl. Pharmacol.* **2004**, *199*, 316–331. [CrossRef] [PubMed]
51. McLean, L.; Soto, U.; Agama, K.; Francis, J.; Jimenez, R.; Pommier, Y.; Sowers, L.; Brantley, E. Aminoflavone induces oxidative DNA damage and reactive oxidative species-mediated apoptosis in breast cancer cells. *Int. J. Cancer* **2008**, *122*, 1665–1674. [CrossRef]
52. Panigrahy, D.; Kaipainen, A.; Greene, E.R.; Huang, S. Cytochrome P450-derived eicosanoids: The neglected pathway in cancer. *Cancer Metastasis Rev.* **2010**, *29*, 723–735. [CrossRef] [PubMed]
53. Li, Z.; Chen, G.; Cai, Z.; Dong, X.; He, L.; Qiu, L.; Zeng, Y.; Liu, X.; Liu, J. Profiling of hepatocellular carcinoma neoantigens reveals immune microenvironment and clonal evolution related patterns. *Chin. J. Cancer Res.* **2021**, *33*, 364–378. [CrossRef] [PubMed]
54. Vitale, I.; Sistigu, A.; Manic, G.; Rudqvist, N.P.; Trajanoski, Z.; Galluzzi, L. Mutational and Antigenic Landscape in Tumor Progression and Cancer Immunotherapy. *Trends Cell Biol.* **2019**, *29*, 396–416. [CrossRef] [PubMed]
55. Brodeur, C.M.; Thibault, P.; Durand, M.; Perreault, J.P.; Bisaillon, M. Dissecting the expression landscape of cytochromes P450 in hepatocellular carcinoma: Towards novel molecular biomarkers. *Genes Cancer* **2019**, *10*, 97–108. [CrossRef]
56. Koh, W.P.; Yuan, J.M.; Wang, R.; Govindarajan, S.; Oppenheimer, R.; Zhang, Z.Q.; Yu, M.C.; Ingles, S.A. Aromatase (CYP19) promoter gene polymorphism and risk of nonviral hepatitis-related hepatocellular carcinoma. *Cancer* **2011**, *117*, 3383–3392. [CrossRef]
57. Belboul, A.; Ashworth, J.; Fadel, A.; McLoughlin, J.; Mahmoud, A.; El Mohtadi, M. Estrogen induces the alternative activation of macrophages through binding to estrogen receptor-alpha. *Exp. Mol. Pathol.* **2025**, *143*, 104971. [CrossRef]
58. Bengtsson, A.K.; Ryan, E.J.; Giordano, D.; Magaletti, D.M.; Clark, E.A. 17beta-estradiol (E2) modulates cytokine and chemokine expression in human monocyte-derived dendritic cells. *Blood* **2004**, *104*, 1404–1410. [CrossRef]
59. Nadkarni, S.; McArthur, S. Oestrogen and immunomodulation: New mechanisms that impact on peripheral and central immunity. *Curr. Opin. Pharmacol.* **2013**, *13*, 576–581. [CrossRef]
60. Polanczyk, M.J.; Hopke, C.; Vandenbark, A.A.; Offner, H. Estrogen-mediated immunomodulation involves reduced activation of effector T cells, potentiation of Treg cells, and enhanced expression of the PD-1 costimulatory pathway. *J. Neurosci. Res.* **2006**, *84*, 370–378. [CrossRef]

61. Guo, Y.; Lee, Y.C.; Brown, C.; Zhang, W.; Usherwood, E.; Noelle, R.J. Dissecting the role of retinoic acid receptor isoforms in the CD8 response to infection. *J. Immunol.* **2014**, *192*, 3336–3344. [CrossRef]
62. Manicassamy, S.; Pulendran, B. Retinoic acid-dependent regulation of immune responses by dendritic cells and macrophages. *Semin. Immunol.* **2009**, *21*, 22–27. [CrossRef]
63. Raverdeau, M.; Mills, K.H. Modulation of T cell and innate immune responses by retinoic Acid. *J. Immunol.* **2014**, *192*, 2953–2958. [CrossRef] [PubMed]
64. Farazuddin, M.; Ludka, N.; Friesen, L.; Landers, J.J.; O'Konek, J.J.; Kim, C.H.; Baker, J.R. Retinoic Acid Signaling Is Required for Dendritic Cell Maturation and the Induction of T Cell Immunity. *ImmunoHorizons* **2023**, *7*, 480–492. [CrossRef] [PubMed]
65. Gilardi, F.; Mitro, N.; Godio, C.; Scotti, E.; Caruso, D.; Crestani, M.; De Fabiani, E. The pharmacological exploitation of cholesterol 7alpha-hydroxylase, the key enzyme in bile acid synthesis: From binding resins to chromatin remodelling to reduce plasma cholesterol. *Pharmacol. Ther.* **2007**, *116*, 449–472. [CrossRef]
66. Chen, X.; Yang, D.; Shen, W.; Dong, H.F.; Wang, J.M.; Oppenheim, J.J.; Howard, M.Z. Characterization of chenodeoxycholic acid as an endogenous antagonist of the G-coupled formyl peptide receptors. *Inflamm. Res.* **2000**, *49*, 744–755. [CrossRef]
67. Chiang, J.Y.L.; Ferrell, J.M. Bile acid receptors FXR and TGR5 signaling in fatty liver diseases and therapy. *Am. J. Physiol. Gastrointest. Liver Physiol.* **2020**, *318*, G554–G573. [CrossRef] [PubMed]
68. Godlewska, U.; Bulanda, E.; Wypych, T.P. Bile acids in immunity: Bidirectional mediators between the host and the microbiota. *Front. Immunol.* **2022**, *13*, 949033. [CrossRef]
69. Lin, B.S.; Yin, M.Y.; Xie, S.A.; Li, P.; Li, X. Pleiotropic immunoregulation by bile acids in pathophysiology. *Front. Immunol.* **2026**, *17*, 1719092. [CrossRef]
70. Ma, C.; Han, M.; Heinrich, B.; Fu, Q.; Zhang, Q.; Sandhu, M.; Agdashian, D.; Terabe, M.; Berzofsky, J.A.; Fako, V.; et al. Gut microbiome-mediated bile acid metabolism regulates liver cancer via NKT cells. *Science* **2018**, *360*, eaan5931. [CrossRef]
71. Wang, L.; Gong, Z.; Zhang, X.; Zhu, F.; Liu, Y.; Jin, C.; Du, X.; Xu, C.; Chen, Y.; Cai, W.; et al. Gut microbial bile acid metabolite skews macrophage polarization and contributes to high-fat diet-induced colonic inflammation. *Gut Microbes* **2020**, *12*, 1819155. [CrossRef] [PubMed]
72. Wei, H.; Suo, C.; Gu, X.; Shen, S.; Lin, K.; Zhu, C.; Yan, K.; Bian, Z.; Chen, L.; Zhang, T.; et al. AKR1D1 suppresses liver cancer progression by promoting bile acid metabolism-mediated NK cell cytotoxicity. *Cell Metab.* **2025**, *37*, 1103–1118.E7. [CrossRef]
73. Kivistö, K.T.; Niemi, M.; Schaeffeler, E.; Pitkälä, K.; Tilvis, R.; Fromm, M.F.; Schwab, M.; Eichelbaum, M.; Strandberg, T. Lipid-lowering response to statins is affected by CYP3A5 polymorphism. *Pharmacogenetics* **2004**, *14*, 523–525. [CrossRef]
74. Huang, H.; Zhou, J.; Chen, H.; Li, J.; Zhang, C.; Jiang, X.; Ni, C. The immunomodulatory effects of endocrine therapy in breast cancer. *J. Exp. Clin. Cancer Res.* **2021**, *40*, 19. [CrossRef] [PubMed]
75. Thompson, D.J.; O'Mara, T.A.; Glubb, D.M.; Painter, J.N.; Cheng, T.; Folkerd, E.; Doody, D.; Dennis, J.; Webb, P.M.; Gorman, M.; et al. CYP19A1 fine-mapping and Mendelian randomization: Estradiol is causal for endometrial cancer. *Endocr.-Relat. Cancer* **2016**, *23*, 77–91. [CrossRef]
76. Grindstad, T.; Skjefstad, K.; Andersen, S.; Ness, N.; Nordby, Y.; Al-Saad, S.; Fismen, S.; Donnem, T.; Khanehkenari, M.R.; Busund, L.T.; et al. Estrogen receptors α and β and aromatase as independent predictors for prostate cancer outcome. *Sci. Rep.* **2016**, *6*, 33114. [CrossRef] [PubMed]
77. Kanda, S.; Tsuchiya, N.; Narita, S.; Inoue, T.; Huang, M.; Chiba, S.; Akihama, S.; Saito, M.; Numakura, K.; Tsuruta, H.; et al. Effects of functional genetic polymorphisms in the CYP19A1 gene on prostate cancer risk and survival. *Int. J. Cancer* **2015**, *136*, 74–82. [CrossRef]
78. Aragon-Ching, J.B.; Williams, K.M.; Gulley, J.L. Impact of androgen-deprivation therapy on the immune system: Implications for combination therapy of prostate cancer. *Front. Biosci.* **2007**, *12*, 4957–4971. [CrossRef]
79. Sommer, U.; Ebersbach, C.; Beier, A.K.; Baretton, G.B.; Thomas, C.; Borkowetz, A.; Erb, H.H.H. Influence of Androgen Deprivation Therapy on the PD-L1 Expression and Immune Activity in Prostate Cancer Tissue. *Front. Mol. Biosci.* **2022**, *9*, 878353. [CrossRef]
80. Dyhl-Polk, A.; Mikkelsen, M.K.; Ladekarl, M.; Nielsen, D.L. Clinical Trials of Immune Checkpoint Inhibitors in Hepatocellular Carcinoma. *J. Clin. Med.* **2021**, *10*, 2662. [CrossRef]
81. Cheng, A.L.; Qin, S.; Ikeda, M.; Galle, P.R.; Ducreux, M.; Kim, T.Y.; Lim, H.Y.; Kudo, M.; Breder, V.; Merle, P.; et al. Updated efficacy and safety data from IMbrave150: Atezolizumab plus bevacizumab vs. sorafenib for unresectable hepatocellular carcinoma. *J. Hepatol.* **2022**, *76*, 862–873. [CrossRef]
82. Guo, Y.; Pan, Z.; Kan, X.; Li, T.; Gong, B.; Li, Y.; Yang, L.; Zheng, C. Immunotherapy improved the efficacy of TACE or TACE plus MTTs in HCC patients: A meta-analysis. *Int. Immunopharmacol.* **2025**, *147*, 114006. [CrossRef] [PubMed]
83. Barjij, I.; Meliani, M. Immunogenic Cell Death as a Target for Combination Therapies in Solid Tumors: A Systematic Review Toward a New Paradigm in Immuno-Oncology. *Cureus* **2025**, *17*, e85776. [CrossRef]
84. Dou, L.; Fang, Y.; Yang, H.; Ai, G.; Shen, N. Immunogenic cell death: A new strategy to enhancing cancer immunotherapy. *Hum. Vaccines Immunother.* **2024**, *20*, 2437918. [CrossRef] [PubMed]

85. Li, C.; Qi, X.; Yan, M. Chemotherapy-induced immunogenic cell death in combination with ICIs: A brief review of mechanisms, clinical insights, and therapeutic implications. *Front. Pharmacol.* **2025**, *16*, 1572195. [CrossRef]
86. Özkan, A.; Stolley, D.L.; Cressman, E.N.K.; McMillin, M.; DeMorrow, S.; Yankeelov, T.E.; Rylander, M.N. Tumor Microenvironment Alters Chemoresistance of Hepatocellular Carcinoma Through CYP3A4 Metabolic Activity. *Front. Oncol.* **2021**, *11*, 662135. [CrossRef]
87. Aoki, T.; Nishida, N.; Kurebayashi, Y.; Sakai, K.; Fujiwara, N.; Tsurusaki, M.; Hanaoka, K.; Morita, M.; Chishina, H.; Takita, M.; et al. Molecular classification of hepatocellular carcinoma based on zoned metabolic feature and oncogenic signaling pathway. *Clin. Mol. Hepatol.* **2025**, *31*, 981–1002. [CrossRef]
88. Qin, R.; Jin, T.; Xu, F. Biomarkers predicting the efficacy of immune checkpoint inhibitors in hepatocellular carcinoma. *Front. Immunol.* **2023**, *14*, 1326097. [CrossRef] [PubMed]
89. Ye, L.; Yang, X.; Guo, E.; Chen, W.; Lu, L.; Wang, Y.; Peng, X.; Yan, T.; Zhou, F.; Liu, Z. Sorafenib metabolism is significantly altered in the liver tumor tissue of hepatocellular carcinoma patient. *PLoS ONE* **2014**, *9*, e96664. [CrossRef]
90. Zhang, Y.; Wang, Z.; Wang, Y.; Jin, W.; Zhang, Z.; Jin, L.; Qian, J.; Zheng, L. CYP3A4 and CYP3A5: The crucial roles in clinical drug metabolism and the significant implications of genetic polymorphisms. *PeerJ* **2024**, *12*, e18636. [CrossRef]
91. Liu, L.; Mo, M.; Chen, X.; Chao, D.; Zhang, Y.; Chen, X.; Wang, Y.; Zhang, N.; He, N.; Yuan, X.; et al. Targeting inhibition of prognosis-related lipid metabolism genes including CYP19A1 enhances immunotherapeutic response in colon cancer. *J. Exp. Clin. Cancer Res.* **2023**, *42*, 85. [CrossRef]
92. Tong, Y.; Lou, X. Interplay between bile acids, gut microbiota, and the tumor immune microenvironment: Mechanistic insights and therapeutic strategies. *Front. Immunol.* **2025**, *16*, 1638352. [CrossRef]
93. Varanasi, S.K.; Chen, D.; Liu, Y.; Johnson, M.A.; Miller, C.M.; Ganguly, S.; Lande, K.; LaPorta, M.A.; Hoffmann, F.A.; Mann, T.H.; et al. Bile acid synthesis impedes tumor-specific T cell responses during liver cancer. *Science* **2025**, *387*, 192–201. [CrossRef]
94. Chen, F.; Cai, Y.; Zhou, J. Relationship between retinol metabolism and hepatocellular carcinoma: A comprehensive analysis of Mendelian randomization, prognostic characteristic and experiment. *Discov. Oncol.* **2025**, *16*, 513. [CrossRef]
95. Nelson, C.H.; Buttrick, B.R.; Isoherranen, N. Therapeutic potential of the inhibition of the retinoic acid hydroxylases CYP26A1 and CYP26B1 by xenobiotics. *Curr. Top. Med. Chem.* **2013**, *13*, 1402–1428. [CrossRef]
96. Bi, G.; Liang, J.; Bian, Y.; Shan, G.; Besskaya, V.; Wang, Q.; Zhan, C. The immunomodulatory role of all-trans retinoic acid in tumor microenvironment. *Clin. Exp. Med.* **2023**, *23*, 591–606. [CrossRef]
97. Li, X.; Luo, X.; Chen, S.; Chen, J.; Deng, X.; Zhong, J.; Wu, H.; Huang, X.; Wang, C. All-trans-retinoic acid inhibits hepatocellular carcinoma progression by targeting myeloid-derived suppressor cells and inhibiting angiogenesis. *Int. Immunopharmacol.* **2023**, *121*, 110413. [CrossRef]

Disclaimer/Publisher's Note: The statements, opinions and data contained in all publications are solely those of the individual author(s) and contributor(s) and not of MDPI and/or the editor(s). MDPI and/or the editor(s) disclaim responsibility for any injury to people or property resulting from any ideas, methods, instructions or products referred to in the content.